LA-UR- 09-00920

Approved for public release;
distribution is unlimited.

Title:	THE MECHANICAL RESPONSE OF A URANIUM-NIOBIUM ALLOY: A COMPARISON OF CAST VERSUS WROUGHT PROCESSING
Author(s):	Carl M.Cady, G.T. Gray III, S.R. Chen, E.K. Cerreta, C.P. Trujillo, M.F. Lopoz, R.M. Aikin, D.R. Korzekwa, and A.M. Kelly
Intended for:	DYMAT 2009 SEPT 7-11, 2009 Brussels, Belgium

Form 836 (7/06)

The Mechanical Response of a Uranium-Niobium Alloy: A Comparison of Cast Versus Wrought Processing

C.M. Cady[1], G.T. Gray III[1], S.R. Chen[1], E.K. Cerreta[1], C.P. Trujillo[1], M.F. Lopez[1], R.M. Aikin[2], D.R. Korzekwa[2], and A. M. Kelly[2]

[1]*MST-8, MS G-755, Los Alamos National Laboratory, Los Alamos, NM 87545, U.S.A.*
[2]*MST-6, MS G-770, Los Alamos National Laboratory, Los Alamos, NM 87545, U.S.A.*

Abstract. A rigorous experimentation and validation program is being undertaken to create constitutive models that elucidate the fundamental mechanisms controlling plasticity in uranium-6 wt.% niobium alloys (U-6Nb). The first, "wrought", material produced by processing a cast ingot via forging and forming into plate was studied. The second material investigated is a direct cast U-6Nb alloy. The purpose of the investigation is to determine the principal differences, or more importantly, similarities, between the two materials due to processing. It is well known that parameters like grain size, impurity size and chemistry affect the deformation and failure characteristics of materials. Metallography conducted on these materials revealed that the microstructures are quite different. Characterization techniques like tension, compression, and shear were performed to find the principal differences between the materials as a function of stress state. Dynamic characterization using a split Hopkinson pressure bar in conjunction with Taylor impact testing was conducted to derive and thereafter validate constitutive material models. The Mechanical Threshold Strength Model is shown to accurately capture the constitutive response of these materials and Taylor cylinder tests are used to provide a robust way to verify and validate the constitutive model predictions of deformation by comparing finite element simulations with the experimental results. The primary differences between the materials will be described and predictions about material behavior will be made.

1. INTRODUCTION

The primary reason for the work presented in this paper is to: 1) develop the selection criteria for choosing suitable replacement materials, and 2) implement a strategy that investigates the requirements necessary for material replacement. For example, in this case, it is necessary that the replacement material maintain its corrosion resistance, density and mechanical properties. The goal, therefore, was to develop a process that produced the same alloy in a more reliable, cost and time efficient manner. It is known that niobium alloying affects the phase stability, mechanical properties and deformation mechanisms of the material. The presence and stability of martensite, deformation by twinning, and solute homogeneity are all known to influence the plastic and elastic stress/strain behavior of the U-Nb alloys [1]. It is also well understood that significant changes in processing generally lead to changes in microstructure, i.e. grain size, inclusion size and density, anisotropy, and substructure. These properties, in turn, influence the elastic and plastic behavior. Therefore, it is necessary to di-

rectly compare results of pertinent experiments in order to make judgments on the suitability of replacement materials.

In order to determine if cast is a suitable replacement it is necessary to quantify differences between wrought and cast U-6Nb materials. This will be done by observing the microstructure using optical and scanning electron microscopy (SEM), and by analyzing stress-strain behavior as a function of temperature and strain rate. It is also necessary and develop a constitutive model for cast U-6Nb and compare it to the wrought material. The wrought alloy is produced through a process where it was vacuum induction melted, arc-skull melted, and vacuum arc re-melted and cut into ingots. The ingot is then forged, rolled and formed in the high-temperature γ body-centered cubic (bcc) phase field (above 900°C). The cast material was created by vacuum induction melting and then shape casting. At this point both materials are processed further by vacuum solution heat treat (850°C) for 1 hour to put the niobium into solid solution and to remove hydrogen. Then it is oil quenched to room temperature at rates greater than 20 °C /second. The high quench rate is required to by-pass the more brittle equilibrium phases to form the metastable α" (U-6Nb) martensite phase [1,2], and then final machining. The α" phase is required to obtain the corrosion resistant properties, owing to the supersaturation of Nb in the structure as well as the lower yield strength and higher ductility associated with the shape memory effect (SME) deformation mechanisms exhibited by the α" martensite. A detailed investigation of the deformation in this alloy was carried out by Field [3-5] describing the dominant deformation processes during both SME and post-SME deformation. Niobium concentration ranging from 4.5 to 7.5 wt % are common in the wrought alloy and niobium variations in the cast alloy range from 5.5 to 6.3 wt %. Because of the tendency for segregation in this alloy there is the potential for some untransformed γ^o phase to be retained in the α" in regions that are higher in niobium. Although the Nb variation is narrower in the cast material it is not random. Grain size and niobium concentrations are correlated to the solidification rate in the cast alloy. Smaller grains having lower niobium compositions are found where the casting first solidifies and larger grains with higher niobium concentration are found in regions of last solidification.

2. EXPERIMENTAL TECHNIQUES

Metallography was conducted on the wrought and cast materials to determine the initial characteristics of the alloys. The average grain size of the wrought alloy was ~ 50μm diameter with indication of inclusions of the order of ~ 10 μm located at grain boundaries and within grains (Fig. 1a). The direct cast U-6Nb alloy was poured into forms that were nominally 0.25" thick. The average grain size of the cast material was 300 μm diameter with an average inclusion size of ~ 8-10 μm diameter (Fig.1b).

Following heat treatment, sample blanks were removed from the wrought and cast plates using a wire EDM. These sample blanks were machined into test samples using conventional milling and turning with carbide tooling. The mechanical response of the U-6Nb alloys was measured in compression using solid cylindrical samples nominally 5 mm in diameter by 5 mm in length. Molybdenum disulfide spray was used to lubricate the specimen ends in all samples tested above -40°C. Boron nitride spray was used to lubricate the specimen ends at lower temperatures. Quasi-static compression tests were conducted at rates of 10^{-3}/s and 1/s between -188°C to 21°C in air using a hydraulic MTS 880 load frame with highly polished tungsten carbide platens. Temperature control was carried out using either electrically heated or liquid nitrogen cooled platens and surrounding insulation was used to isolate the sample. The samples were allowed to equilibrate at temperature for 10 minutes prior to testing. Dynamic tests at strain rates of 1500 to 4000/s were conducted on a split Hopkinson pressure bar [6] fitted with a small chamber around the sample that allowed for testing from -100°C to 400°C in vacuum. For experiments up to 200°C the test duration was 15 minutes with the sample held at temperature at least 10 minutes. Characterization of the materials above 200°C with a dwell prior to testing resulted in significant age hardening so the thermal heating profile was adjusted to test the ma-

terial at temperature without the soak time. Elevated temperature tests were conducted using a resistance furnace with a heating rate of 100°C/minute. Low temperature tests were carried out by blowing evaporated liquid nitrogen into the chamber and around the sample. The validity of each Hopkinson bar test was determined by established criteria [6]. For the geometry of the test samples, stress state equilibrium was achieved at ~4% true strain. The inherent oscillations in the dynamic stress-strain curves and the lack of stress equilibrium in the specimens at low strains make the determination both of the lower and upper yield inaccurate at high strain rates [6-8]. Tensile samples were machined to have a gauge length of 18 mm and 3 mm diameter. Tests were conducted at a true strain rate of 10^{-3}/s and at a temperature of 21°C. The modulus and the strain values were measured using a clip-on extensometer with a 12.7 mm gage length. In addition to traditional tensile and compression testing, forced shear tests were performed on both materials. The specimen geometry consists of a cylindrical hat shaped specimen in which the outer diameter (~ 4.6 mm) of the hat is larger than the inner diameter of the brim (~ 4.2 mm) with a gauge length of (~ 0.9 mm) [9]. The result is that rather than a pure shear loading, there is a hoop stress exerted on the gauge section. These specimens were loaded at room temperature at 0.001/s. Data from these tests in converted from load-displacement to engineering stress/displacement data by simply resolving the load onto the plane of shear. Displacement represents the vertical displacement in mm of the specimen. Finally, Taylor impact experiments will be conducted using samples that are 7.62 mm diameter. The wrought materials had an average length of 50mm and the cast material length was 38 mm. Samples were tested to determine the maximum velocity without causing failure. Diagnostics on this test include measurement of exist velocity and high speed photography of the round impacting the anvil.

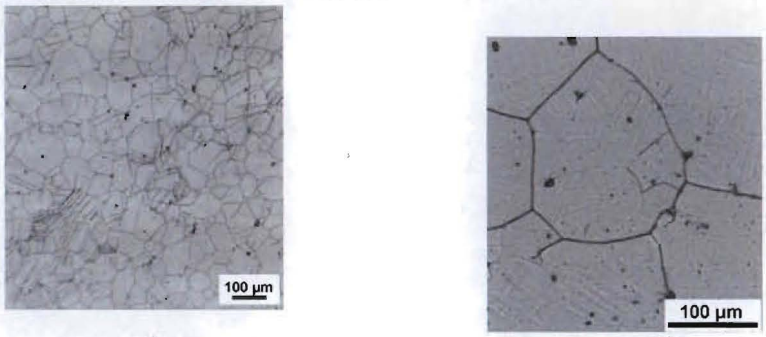

a) b)

Figure 1: Starting mictostructures of the a) wrought U-6Nb alloy and b) cast alloy

3. RESULTS AND DISCUSSION

The influence of temperature and strain rate on the compressive mechanical behavior of both wrought and cast U-6wt % Nb is presented in Figures 2a and 2b. General comments pertaining to both materials are: 1) Decreasing the temperature for a constant strain rate shifts the lower and upper yield points to higher stresses. 2) The work hardening rates are parallel for low strain rate tests, especially at strains greater than 7%. 3) For a given temperature, the work hardening rate will decrease with increasing strain rate. This is caused by adiabatic heating and can be clearly seen when one compares the amount of upward shift upon reloading for tests at 0.001/s and 1/s and a temperature of -40°C. 4) The work hardening rates at 21°C for the strain rates presented are nearly parallel above 7% strain.

This constitutive response is consistent with materials whose mechanical behavior is dominated by a strong Peierls stress [7]. Comparing the two materials at lower strain rates (Fig 2a) it is seen that the cast materials has a similar overall flow behavior to the wrought material but the slightly higher slope of the work hardening of the cast material may be related to the inclusions size and concentration. For the tests that show adiabatic heating there also seems to nearly the same increase in strength

(~200 MPa for the cast material and ~160 MPa for the wrought material) so this comparison indicates the these materials behave similarly, but that the internal heating may be higher in the cast material. There is indication of adiabatic heating in the cast material at low strain rate (0.001/s) at room temperature and below but the wrought material did not show this at 21°C and had only a small increase in strength at -40°C (~25 MPa). It has also been observed that the loading modulus is significantly lower than the unloading modulus. This is attributed to the deformation mechanisms activated during the initial loading. The early deformation is dominated by twinning and produces a modulus value that ranges from ~ 11 GPa to 18 GPa depending on sample preparation and subsequent heat treatments. It is important to note that the modulus value is estimated from the region that appears to be the most linear in load/displacement. However, there is evidence that there is no truly elastic deformation in this material. Rather, it is known that plastic deformation is initiated from the onset of loading [10].

A results of the high strain rate tests as a function of temperature that were run on both materials under conditions that would minimize the age hardening effects are presented in Figure 2b. The initial "elastic" loading and lower yield behavior only represent transient behavior and should only be interpreted as depicting the classic shape memory behavior without reporting any specific stress or strain values. The two materials exhibit little difference at strain rates above ~ 1400/s and variation in the test temperature could account for the minor difference between the cast and wrought at 400°C.

The Figure 2c shows the true stress true strain curves for the tensile tests. The primary difference between the two materials is the behavior near the second yield point. For the wrought material the stress-strain response has a slight inflection indicating a higher contribution from twinning, which is supported by calculations of resolved shear stresses for potential post-SME deformation systems based on a single crystal model [5] (a gross simplification of the polycrystalline material) followed by dislocation dominated deformation. Because the cast material does not exhibit the inflection after the second yield seen in the wrought material it appears that the work hardening behavior is dominated by dislocation deformation and that there is little or no twin dominated deformation. Further microscopic evaluation of the cast material is necessary in order to determine the governing deformation mechanism.

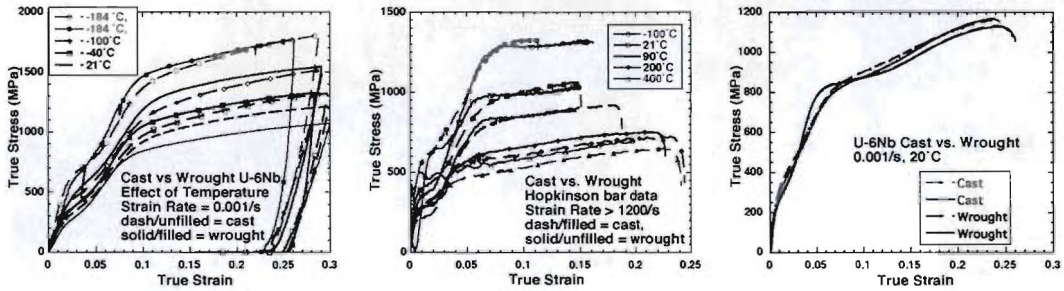

a) b) c)

Figure 2: Compression and tensile test results of cast and wrought U-6Nb alloys: a) as a function of temperature at low strain rate, b) as a function of temperature for SHPB experiments, and c) for tensile tests at room temperature and low strain rate..

Rapid changes in texture in the post-SME regime are consistent with twining contributions to deformation for both tension and compression, however. One difference that can be observed in Figure 2a and 2c is that the transition occurs at different strains for compression versus tension. Again, the single crystal model can potentially provide insight into this behavior, since the martensite transformations strains (from which variant switching accommodation strains are derived) are slightly higher for compression [5] and the resolved shear stresses for post-SME twinning are somewhat higher for tension. However, a polycrystalline model is needed to properly address these effects. The modulus of the material is also higher in tension than in compression. This may be related to increased variant switching accommodation strains in compression.

The shear top hat test data for both the cast and wrought specimens is given in Figure 3a. The behavior of the two materials is similar with the small exception that the cast material seems to be more stable in shear than the wrought material. The cast material in this set of experiments did not actually begin to shear band, which would be indicated in the mechanical test data by a sudden, precipitous drop in the stress. Instead, the sample response displays hardening behavior and then unloading. Figure 3b shows metallography of a wrought top hat specimens sectioned parallel to the loading axis. It can be seen that the specimen has almost completely failed due to cracking along the shear band in the gauge section by a displacement of 0.304 mm. From the mechanical test data, Figure 3a, as well as the metallography it appears that failure is an abrupt event rather than a continuous deformation process, as there was almost no deformation observed in a specimen deformed to 0.107mm displacement. Figure 3c shows the optical metallography of the cast top hat specimens sectioned parallel to the loading axis having a displacement of 0.277 mm (As Cast 1). It can be seen that these specimens have not failed and that a much larger grain size exists in the cast material as compared to the wrought material. This may be why more twinning is observed in the cast versus the wrought material.

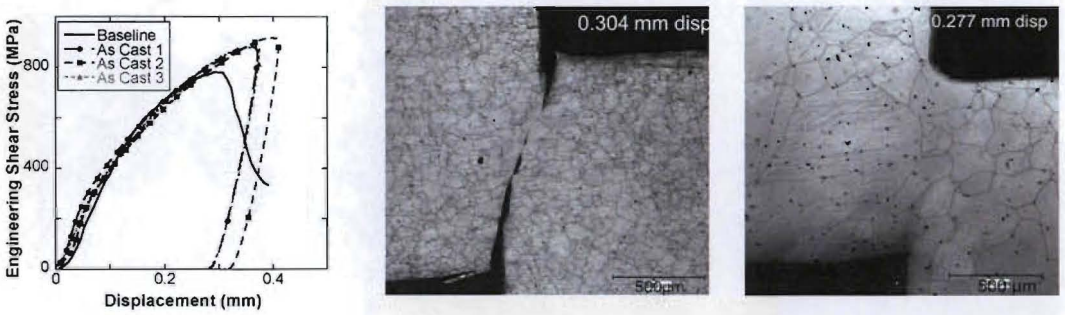

.a) b) c)

Figure 3: Shear loading results for Cast and wrought U-6Nb. A) The Shear strength versus verticle displacement, b) Micrograph of the shear localization for wrought material showing the failure crack, c) Tht cast material with similar displacement showing little indication of localization or failure.

The property that is of interest for the Taylor impact experiments is related to the fracture strength. i.e. what velocity or kinetic energy (1/2 mv^2) is required to cause the sabot to fragment. The most direct method of comparison between materials would be to compare velocities at which fragmentation initiates. However, as the samples had different lengths the best way to compare these test results is to calculate the kinetic energy at impact. However, this comparison neglects the effects of friction and the differences in ductility between the materials. Experiments show that the cast material can impact the surface with an energy of ~255 J and remain intact. The wrought material can impact with a kinetic energy of ~350 J and remain intact.

The MTS parameter set generated in 2004 for wrought U-6wt%Nb was used to compare the cast and wrought materials investigated in this study. The strength at 20% of strains shows a three fold increase from high temperature (400°C) to the low temperature test at -184°C this behavior indicates a high-temperature sensitivity of the material. The MTS parameters derived for the wrought U-6wt%Nb were used to calculate the mechanical responses for each testing condition in current experimental matrix and the comparisons between model and experimental data were made. The initial loading portion as a result of twinning/martensitic transformation was not reproduced in the model and the focus was concentrated to describe the mechanical response after the transformation was complete. Initial comparisons of the tests showed very good agreement with two tests at strain rate of 1/s at 233K and 294K providing an initial validation the effect of temperature softening due to adiabatic heating. The calculated adiabatic data trace the experimental measurement very well, and the calculated isothermal responses capture the strength level at reloading exactly. It is determined from this comparison that the MTS parameters validated against a Taylor cylinder test for the wrought material works well for the

cast material.

4. SUMMARY AND CONCLUSIONS

The current investigation compares cast and wrought U-6Nb. Specific conclusions of this work are as follows.

1) To a first approximation, cast U-6Nb has the same tensile and compressive behavior as wrought U-6Nb. This similarity is likely attributed to the twin substructure within the grains of both materials and not on the prior gamma grain structures that are seen to be significantly different.
2) Shear localization occurs in the top hat specimen as tested for wrought material but there is no evidence of the localization in the cast material tested under the same conditions.
3) Without adjusting any parameters in the MTS model of wrought material, it is seen that the calculated stress/strain data follow the experimental data of cast material extremely well.

Experiments to characterize the bi-axial behavior and shear localization behavior at high strain rates are planned in order to fully investigate the importance of stress state and shear localization and failure.

Acknowledgments

This research was supported under the auspices of the US Department of Energy.

References:

[1] R.J. Jackson, "Elastic, Plastic and Strength Properties of U-Nb and U-Nb-Zr Alloys," in Physical Metallurgy of Uranium Alloys, J.J. Burke *et al.*, Eds. (Brook Hill, Boston, MA, 1976) pp. 611-657.
[2] K.H. Eckelmeyer, "Aging Phenomena in Dilute Uranium Alloys," in Physical Metallurgy of Uranium Alloys, J.J. Burke *et al.*, Eds., (Brook Hill, Boston, MA, 1976) pp. 463-509.
[3] R.D. Field, D.J. Thoma, P.S. Dunn, D.W. Brown and C.M. Cady, *Phil. Mag. A* **81**, 7 (2001) pp. 1691-1724.
[4] R.D. Field, D.W. Brown, and D.J. Thoma, *Phil. Mag. A* **85**, 23 (2005) pp. 2593-2609.
[5] R.D. Field, D.W. Brown, and D.J. Thoma, in Proceedings of the International Conference on Solid- Solid Phase Transformations in Inorganic Materials 2005 (PTM 2005), Vol. 2, J.M. Howe, et al. eds., (TMS, Warrendale, PA, 2005) pp. 227-232.
[6] G.T. Gray III, " Mechanical Testing and Evaluation, " in ASM Metals Handbook Volume 8, edited by H. Kuhn and D. Medlin, (ASM International, Metals Park, Ohio 44073-0002, 2000) pp. 462–476
[7] S.R. Chen and G.T. Gray III, (1996) *Met. Trans. A*, Vol. **27A** (1996) pp. 2994-3006
[8] P.E. Armstrong, "High Strain Rate Mechanical Behavior," in Metallurgical Technology of Uranium and Uranium Alloys, (ASM, Metals Park, Ohio, 1982) pp. 295-342,.
[9] Q. Xue, G.T. Gray III, B.L. Henrie, S.A. Malloy, and S.R.Chen, *Met. Trans. A*, Vol. **36A** (2005) pp. 1471-1486
[10] C.M. Cady, G.T. Gray III, S.R. Chen, R.D. Field, D.R. Korzekwa, R.S. Hixson, and M.F. Lopez, *J. Phys IV* **134** (2006) 203-208